

Ergonomic and mathematical approach to wire-driven parallel haptic interfaces

Carlos González¹
Universidad
Politécnica de
Madrid

Manuel Ferre²
Universidad
Politécnica de
Madrid

Roque Saltarén³
Universidad
Politécnica de
Madrid

Jordi Barrio⁴
Universidad
Politécnica de
Madrid

Rafael Aracil⁵
Universidad
Politécnica de
Madrid

Juan M. Ibarra⁶
Cinvestav

ABSTRACT

The aim of this paper is the design and the analysis of the workspace of n -DOF (degree of freedom) wire-driven parallel haptic interfaces with $m = (n+1)$ actuators.

A goal of this paper is an innovative approach to the evaluation of the workspace. A key point to consider when evaluating the workspace is the user, both his comfort and forces and posture. These considerations will be applied to planar haptic interfaces ($m = 4$, $n = 3$).

The maximum isotropic wrench (force/torque) will be used as index to evaluate the workspace, since it is not possible using the global condition index (GDI). Some aspects of optimal design of this kind of devices will be tackled: the calculus of forces at each wire, the placement of actuators and wires.

Keywords: wire-driven devices, workspace, comfort, polytop

1 INTRODUCTION

Haptic devices let the user feel, touch and manipulate objects simulated in a virtual environment (VE) or teleoperated environments reflecting wrenches in response to the user's movements and supplying the user a very important information when making a task. These devices can be used in many applications: medical operation support and simulation, mechanical design, maintenance and assembly tasks simulation, entertainment, teleoperation...

When designing a force-feedback device there are two aspects to consider: the device itself and the user and the interaction between both of them.

2 USER CONSIDERATIONS

Regarding to the user there are three aspects, linked one to each other, to consider: the perception of position and exerted forces, the reachable points and upper limb posture and user comfort.

2.1 Perception of position and forces

The perception of our own position, movements and forces is carried out by the kinesthetic sense. The resolution of this sense is not very high (it's not necessary a extremely high position accuracy) and is measured by the just-noticeable-difference (JND) parameter, that values the non-noticeable angle variation of a joint. According to [9] the arm values are: $0,8^\circ$ in the shoulder, $2,0^\circ$ in the elbow, $2,0^\circ$ in the wrist and $2,5^\circ$ in a finger. With regard to sensation of wrenches a human can perceive, several studies [15, 8] have determined a range of resolution

between 0,005 N y 0,01 N. Regarding to the force a user can exert, depends on how objects are grasp. There are two kinds of grip: power grip and precision grip. Figure 1 depicts the different kind of grasp [2].

With power grip a greater stability and force is achieved since the back of the hand is used. In spite of this, tasks are carried out with less dexterity than precision grasp (only the fingers are used).

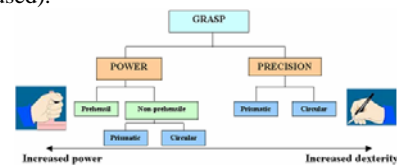


Figure 1 : Power grip vs. precision grip

The ability to grasp an object precisely between the thumb and index finger enables humans to perform a wide range of complex and delicate hand movements. According to latter definitions, the maximum controllable force -grasping with a hand- a man can exert is 400 N, and a woman, 228 N. However, the maximum values, reported by [9], manipulating a pen-shaped handle (precision grip) are: 67 N of maximum static force exerted whilst pinching a 20 mm handle with the thumb in opposition of both the index and middle fingers; and 0,7 N-m of maximum static twisting torque on a circular knob of 20 mm diameter. These values are the maximum ones, but the tolerable continuous force, that is, the force that doesn't produce physical pain nor fatigue in long periods, mustn't exceed ~15% of the maximum values. These values will be taken into consideration when electing the actuators for the device.

2.2 Reachable points and posture

Human joints are composed by bones and ligaments and their movement is provoked by the relative movement of bones. The movement is a composition of rolling and sliding and the instantaneous center of rotation (ICR) is not fixed. However, the locus formed by ICRs are small areas, and the axes of rotation can be considered fixed. Moreover, the most important movement to consider it's the wrist's one, since it limits the most, the user comfort. The wrist is the most complicated joint in the body and his principal movements are the following [6]:

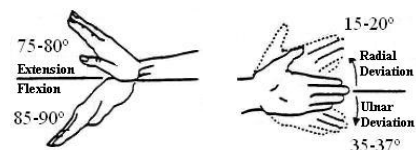


Figure 2 : Main wrist motions

¹ e-mail: cgonzalez@etsii.upm.es
² e-mail: mferre@etsii.upm.es
³ e-mail: rsaltaren@etsii.upm.es
⁴ e-mail: jbarrio@etsii.upm.es
⁵ e-mail: aracil@etsii.upm.es
⁶ e-mail: jibarra@ctrl.cinvestav.mx

- Flexion-Extension. The normal wrist range is 85/90° (flexion) and 75/80 (extension) although it can vary.
- Radial-Ulnar Deviation. The total arc of radial-ulnar deviation is ~50°, 15/20° radially and 35/37° ulnarly.

These values are the maximum a human can reach but the real ones a person can reach in a comfortable fashion are smaller as next section describes.

2.3 User comfort

Bad arm posture affects strength and produce musculoskeletal disorders associated with [3]:

- Forearm pronation
- Radial/Ulnar deviation >15°
- Wrist extension/flexion >20°

Therefore effector should be shaped to avoid wrist deviation, allowing the hand and forearm to remain in alignment during forceful grip exertion. There are several methods to evaluate the ergonomic behavior of a task. The *RULA* method [11] is used here to calculate the maximum joint angles without injuring the user, giving a score depending on loads and posture of the arm, wrist and the general body posture. With the same posture as controlling a mouse and a limitation of deviation of $\pm 15^\circ$ a score of +2 is obtained (acceptable posture). Likewise, the report by [3] shows that the use of a pen-shaped tool instead of a conventional mouse reduces the pronation and the ulnar deviation of the wrist, whereas the task performance remains the same. In order to supply the user the maximum comfort -in a planar interface- the tool must be a pen-shaped effector, that allows gripping in a precision manner and in a comfortable way.



Figure 3 : Pen-shaped tool

2.4 Wire-device considerations

Basic features of haptic devices have been reported widely [4]. The use of wires entails some advantages as low inertia, that improves backdriveability and allows faster movements; large workspace and possible high number of DOF. On the other hand, the use wires has some disadvantages that will be tackled: unidirectional forces and redundancy and calculation of feedback forces.

3 WORKSPACE ANALYSIS

3.1 Isotropic analysis

Workspace of wire-driven haptic interfaces is the volume of the space, the device can exert any kind of wrench in. In robotics GCI (global conditioning index) is usually used to characterize the workspace and the dexterity of the device, however, GCI can't be applied to redundant mechanisms because the condition number expresses no more the relation between extreme forces nor velocities [13]. When considering a redundant device, the jacobian matrix is not square ($J \in \mathcal{R}^{m \times m}$ $m > n$) and last column of the diagonal matrix of the singular value decomposition (SVD) of J is equal to zero, what means a projection of the polytop of force actuator constraints from the m-dimensional to

the n-dimensional space. Figure 4 depicts the transformation with $n=2$ and $m=3$.

The corresponding value to the condition number when considering the polytop is the relation between the greatest and lowest axis of the ellipsoid of maximum surface tangent to the polytop. This value is very complicated to compute and also doesn't give any information of forces values, only the relation between the maximum and minimum one. Therefore, it will be used the method proposed by [14], that is, the use of the maximum isotropic force/torque (MIF) the device can exert in each point. The value of the MIF is the radius of the maximum hypersphere tangent to the polytop in the task space and can be calculated in a easier way.

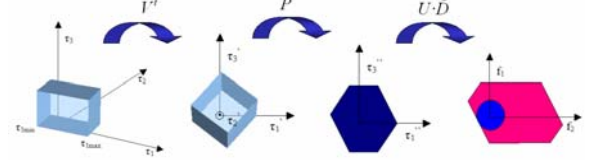


Figure 4 : Polytop transformation

3.2 Calculus of the maximum isotropic force (MIF)

The method proposed by [14] can't be put into practice, specially with a high number of DOF, due to calculation time is high. A much more efficient method that reduces calculation time is presented. The key point is to calculate the possible boundaries (hyperplanes) of the final polytop (task space) as the transformed boundaries of the initial polytop and among these hyperplanes, determinate those that are actually real boundaries. For the sake of the understanding, let's suppose you have 3 actuators ($m = 3$ and $n = 2$) and actuator constraints represent a cube. When projecting it to the task space one obtains a parallelogram. The lines, that are the boundaries of the parallelogram, are the projection of cube's edges. Thus, first the edges of polytop in joint space must be calculated and then they must be mapped to task space.

The edges can be represented by a vector with two fixed coordinates, with value f_{min} or f_{max} , that are the actuators' force limits. So this vector is $\Lambda = (x_1, \dots, f_{min/max}, \dots, x_r, \dots, f_{min/max}, \dots, x_m)$ where x_i can vary. If J is decomposed as follows:

$$F = J^t \cdot \Lambda = J_{1-n}^t \cdot \Lambda_{1-n} + j_m \cdot \lambda_m^1$$

$$J_{1-n}^t \cdot F = \Lambda_{1-n} + J_{1-n}^t \cdot j_m \cdot \lambda_m = \Lambda_{1-n} + \tilde{j}_m \cdot \lambda_m \quad (1)$$

In order to obtain a boundary-hyperplane in task space ($u_k \cdot F = 1$) it's necessary to achieve an equation in which the λ_i variables have been eliminated. This can be done by compounding equations of system (1). There are two possibilities: $\lambda_m = x_i$ or $\lambda_m = f_{min} / \lambda_m = f_{max}$. In first case, the rows of the system of equations (1) with $\lambda_i = f^2$ and $\lambda_j = f$ must be combined to eliminate λ_m .

$$\frac{\left[\left(J_{1-n}^t \right)_i \cdot \tilde{j}_{m_j} - \left(J_{1-n}^t \right)_j \cdot \tilde{j}_{m_i} \right] \cdot F}{f \cdot \tilde{j}_{m_j} - f \cdot \tilde{j}_{m_i}} = 1 \quad \frac{\left[\left(J_{1-n}^t \right)_i \right] \cdot F}{f + f \cdot \tilde{j}_{m_i}} = 1^3$$

In both cases, the four hyperplanes (there are four possibilities of combination of f_{max} and f_{min}), are parallel and therefore, only two of them are capable of being a boundary. In order to know which are the boundaries, the same method as [14], to calculate if an hyperplane is a boundary, is used. A

¹ J_{1-n} is the matrix formed by the columns 1 to n and j_m the m-th column of J . The same notation will be use in the sequel.

² f represents f_{max} or f_{min} .

³ The second subindex is the row of the matrix or vector.

boundary must fulfil one of next equations for every vertex mapped trough $\mathcal{J}^t(A_{ver})$:

$$\Lambda_{ver}^1 \cdot u_k < 1 \dots \Lambda_{ver}^{2^m} \cdot u_k < 1 \quad (C1)$$

$$\Lambda_{ver}^1 \cdot u_k > 1 \dots \Lambda_{ver}^{2^m} \cdot u_k > 1 \quad (C2)$$

In this step, only a point of each of the four hyperplanes is necessary, instead of all vertexes. Next step consists in distinguishing among all resulting hyperplanes, those which are the boundaries according to C1 and C2 (considering now all vertexes), and checking whether the origin is inside the resulting polytop. Finally the MIF is calculated:

$$MIF = \min_{i \in \{1..r\}} \frac{1}{\|u_i\|}$$

Table 1 shows how efficient the new method is and proves its effectiveness when the number of DOF increases. Apart from the number of hyperplanes, the proposed method reduces also the number of other operations.

Table 1: Comparison between methods

	Krut [14]	New method
General	$C_{2^m}^n = \binom{2^m}{n} = \frac{2^m!}{(2^m-n)!n!}$	$4 \frac{m(m-1)}{2}$
3 DOF (m=4,n=3)	560	24
6 DOF (m=7,n=6)	$5,423 \cdot 10^9$	84

4 OPTIMIZATION OF ACTUATORS LOCATION

In following lines a method is shown to decide where to place the motors in order to perform the best features of the device when n+1 actuators and n DOF are considered.

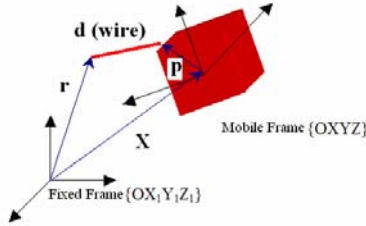


Figure 5 : Scheme of effector and frames

From fig 5 it can be gathered that $d_j = r_j - (X + A \cdot p_j)$ $j = 1 \dots m$ (A , rotation matrix) and wire forces can be expressed as $f_j = \lambda_j d_j / \|d_j\| = \lambda_j du_j$. Torques can be calculated as $t_j = A \cdot p_j \times f_j = A \cdot p_j \times \lambda_j du_j = \lambda_j A \cdot p_j \times du_j$ and finally expressed together:

$$\begin{pmatrix} f \\ t \end{pmatrix} = \begin{pmatrix} du_1 & du_2 & \dots & du_m \\ A \cdot p_1 \times du_1 & A \cdot p_1 \times du_2 & \dots & A \cdot p_m \times du_m \end{pmatrix} \begin{pmatrix} \lambda_1 \\ \vdots \\ \lambda_m \end{pmatrix} = -J^t \cdot \Lambda = M \cdot \Lambda$$

Any wrench (f, t) must be a linear combination of columns of $-J^t = M$, but due to wires only exert traction forces ($\lambda_i > 0$), at least an extra motor is necessary. In order to have a feedback of any wrench (without considering the actuators limitations) it's necessary that a column of matrix M is a negative linear combination of the rest of columns (i.e. the last one): $m_m = m_{n+1} = -\sum \mu_i m_{n+1}$, $\mu_i \geq 0$ and expressed in the local frame:

$$m_m = \begin{pmatrix} du_m \\ p_m \times du_m \end{pmatrix} = \begin{pmatrix} I \\ R_p \end{pmatrix} du_m = -\sum_{i=1}^{m-1} \mu_i m_i = -M_{1:n} \mu_{1:n} \quad (2)$$

Replacing du_m^l in the second part of the equation, it is possible to eliminate it and obtain the equation $L \cdot \mu_{1:n} = 0$:

$$R_p du_m^l = -M_{torque} \mu_{1:n} \Rightarrow R_p (-M_{force} \mu_{1:n}) = -M_{torque} \mu_{1:n}^1$$

$$\left[R_p \cdot M_{force} - M_{torque} \right] \cdot \mu_{1:n} = 0 \Rightarrow L \cdot \mu_{1:n} = 0$$

Matrix L is not square and vector $\mu_{1:n}$ can be divided among independent and dependent variables:

$$L_a \cdot \mu_a = -L_{b-a} \cdot \mu_{b-a} \Rightarrow \mu_a = -L_a^{-1} \cdot L_{b-a} \cdot \mu_{b-a} = -LL \cdot \mu_{b-a}$$

When vector $\mu_{1:n}$ is replaced in equation (2), the vector for last wire is obtained:

$$du_m^l = -M_{force} \begin{pmatrix} -LL \cdot \mu_{b-a} \\ \mu_{b-a} \end{pmatrix} = -M_{force} \begin{pmatrix} -LL \\ I \end{pmatrix} \mu_{b-a} = -M_{force} \cdot C \cdot \mu_{b-a}$$

Expressing vector du_m^l in the global frame a equation that expresses where to place the last engine according to the others is obtained:

$$du_m = A du_m^l = r_m - (X + A p_m) \Rightarrow r_m = X + A p_m - A M_{force} \cdot C \cdot \mu_{b-a} \quad (3)$$

Moreover, another equation must be fulfilled:

$$\mu_a > 0 \Rightarrow \mu_a = -LL \cdot \mu_{b-a} > 0 \quad r_m = X + A p_m - A M_{force} \cdot C \cdot LL^{-1} \mu_{b-a} \quad (4)$$

Equations (3) and (4) represent area constraints on where to place the extra motor, so this motor must be in the area intersection of both constraints. But these constraints vary from one point and orientation to another. With a careful election a motor placement this problem can be solved. Figure 6 shows these constraints when a planar device is considered.

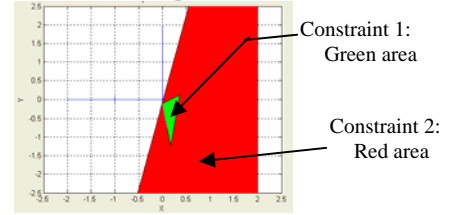


Figure 6 : Area where to place the 4th motor

Another key point to consider is the place where wires connect to the final effector. The experience of [12] about planar wire-devices shows that for effective moments to the human hand, the wires should connect to opposite corners. Now a mathematical approach is shown. As shown before, next equation must be fulfilled:

$$m_m = -\sum_{i=1}^n \mu_i m_i \quad \mu_i \geq 0$$

If vectors m_i are represented in a 3D space (force at the XY plane and torque at Z axis), one can see that last vector must be inside of the convex space determined by the other 3 vectors. In order to get that the fourth vector fulfil this condition when effector spins, it is necessary that the torque component of vectors maintains its sign. To achieve this, the wires must be connected to the effector with a twist, so three of them produce a torque in the same direction and the last one in the opposite (figure 7).

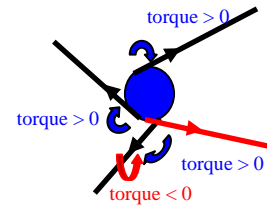


Figure 7 : Connection of wires

¹ M_{force} and M_{torque} are the matrices formed by the rows corresponding to forces or torque respectively.

Finally, last problem to cope with is fixing the force in each wire, once the wrenches on the effector are known. In order to avoid the tedious calculus of the pseudoinverse [12] a new method is proposed. The equation that relates forces is $M \cdot A = F$. Due to M is a $n \times (n+1)$ matrix, n components of Λ can be expressed depending on one λ_i (i.e. λ_m).

$$\begin{aligned} (M_1 \ M_2 \ \dots \ M_n) (\lambda_1 \ \lambda_2 \ \dots \ \lambda_n)^T &= M_{1-n} \cdot \Lambda_{1-n} = F - M_m \cdot \lambda_m \\ \Rightarrow \Lambda_{1-n} &= M_{1-n}^{-1} \cdot F - M_{1-n}^{-1} \cdot M_m \cdot \lambda_m = b - c \cdot \lambda_m \end{aligned}$$

Expressing c as follows, one can see that the components of c correspond to $-\mu_i < 0$ ($c_i = -\mu_i$).

$$M_{1-n} \cdot c = M_m = \sum -\mu_i M_i \quad \mu_i > 0$$

$$Q = \sum \lambda_i = \Lambda_{1-n}^T \{1 \ 1 \ \dots \ 1\}^T + \lambda_m = \sum (b_i - c_i \cdot \lambda_m) + \lambda_m$$

If $Q = 0$ means that some value of λ_i is negative so it's necessary to increase λ_m . Therefore there is a minimum value of λ_m such that, below it, a $\lambda_i < 0$. Thus, to minimize Q , there is a value of λ_m such that all λ_i are positive. That implies that λ_m must be $\lambda_m = \max \{b_i / c_i\}$, that it's the value of λ_i when $\lambda_i = 0$. Thus, to obtain the forces, the system $M \cdot A = F$ must be solved making each time $\lambda_i = 0 \ i=1..m$. Among all the $n+1$ solutions, the proper one is that with all $\lambda_i > 0$ and whose sum of components is minimum.

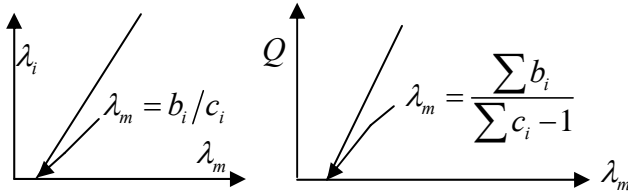


Figure 8 : Wire forces depending on λ_m

For the sake of the performance of the device wires must have a minimum strain ($\lambda_i > \lambda_{\min}$) and the method must be modified slightly. A new variable is created: $\lambda_i' = \lambda_i - \lambda_{\min} > 0 \rightarrow \lambda_i = \lambda_i' + \lambda_{\min}$ and replacing it in equation $M \cdot A = F$:

$$M \cdot (\Lambda' + \Lambda_{\min}) = F \rightarrow M \cdot \Lambda' = F - M \cdot \Lambda_{\min} = F'$$

Latter equation represents an equivalent problem to the first one, so it can be solved as previously explained.

5 PRACTICAL APPLICATION TO A 3-DOF DEVICE

In this section the best configuration, according to the MFI, is shown. The proposed methods have been applied and conditions of human behavior have been taken into account: p coordinates are the way $[a \cdot \cos(\alpha) \ a \cdot \sin(\alpha)]$, where a is equal to 3 cm. for the first 3 points and 12 cm. for the last and α values are $\{80^\circ, 280^\circ, -30^\circ, -100^\circ\}$. The coordinates of r are $\{35 \ 28; \ -35 \ 28; \ -30 \ -25; \ 35 \ -10\}$ (cm.).

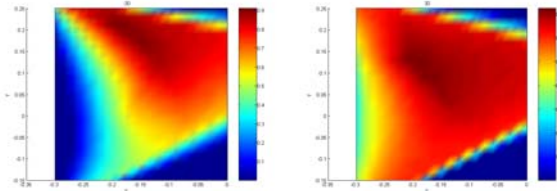


Figure 9 : MFI at extreme twist position ($\pm 30^\circ$)

Figure 9 depicts MIF in each point in the extreme positions, when using the motors: DC, RE-max 24 220428 from Maxon considering a range of 0,2 to 13,3 N. The maximum values are centered on the area where the user is going to move. The mean workspace is a 88 % of a rectangle of 30 x 40 cm. To know the mean values of forces and torques is better not mixing forces and torques, thus making forces or torques equal to zero. When this is made a mean force of 6,42 N and a mean torque of 0,76 N·m are obtained. These are proper values according to the features of the human physiology.

6 CONCLUSION

Design and workspace of wire-driven parallel haptic interfaces have been studied in this paper from a physiological and mathematical point of view. New methods for designing and evaluating the workspace have been presented and all the problems related with this kind of devices were addressed.

REFERENCES

- [1] Anatole Lécuyer, Abderrahmane Kheddar, Sabine Coquillart. A Haptic Prototype for the Simulations of Aeronautics Mounting/Unmounting Operations. IEEE ROMAN'2001, Bordeaux-Paris, France, 18-21.09.2001
- [2] Burdea. G. & Zhuang, J. Dextrous Telerobotics with Force Feedback - an overview. Part 1: Human Factors, Robotica Vol. 9, pp. 171-178. 1991
- [3] Chia-chen Chao and Alan Hedge. Evaluation of Pen-Shaped and Conventional Mouse Designs. Proceedings of the Human Factors and Ergonomics Society 48th Annual Meeting, New Orleans, Sept. 20-24, HFES, Santa Monica, 818-822.
- [4] Cristina Martín Doñate. Interfaces hápticos. Aplicaciones en entornos virtuales. XVI Congreso de Ingeniería Gráfica.
- [5] Daniel J. Schneck and Joseph D. Bronzino. Biomechanics. Principles and applications. CRC Press.
- [6] Daniel M. Sirkett. Prediction of carpal bone kinematics by application of the minimum energy principle. PhD thesis, University Bath, 2001.
- [7] Department of Trade and Industry. Strength Data for design safety. January 2005
- [8] Dhruv, N. y Tendick, F. Frequency Dependence of Compliance Contrast De-tection. Proceedings of the ASME Dynamics Systems and Control Division, DSC-Vol. 69-2, pp. 1087-1093, 2000.
- [9] José María Sabater. Desarrollo de una interfaz kinestésica paralela y experimentación en control de sistemas hápticos y teleoperados. PhD thesis, Universidad Miguel Hernández, 2003. (In spanish).
- [10] Marc Ueberle, Nico Mock, Martin Buss. ViSHaRD10, A Novel Hyper-Redundant Haptic Interface. haptics, pp. 58-65, (HAPTICS'04), 2004.
- [11] McAtamney L., Corlett E.N. RULA: a survey method for the investigation of work-related upper limb disorders. Applied Ergonomics 24 (2), 91-99.
- [12] Robert L. Williams II. CABLE-SUSPENDED HAPTIC INTERFACE. International Journal of Virtual Reality. Vol. 3, No. 3, pp. 13-21. 1998.
- [13] Sébastien Krut, Olivier Company and François Pierrot. Velocity performance indexes for parallel mechanism with actuation redundancy Int. J. of Robotica, Cambridge University Press, Vol. 22, Part 2, March-April 2004.
- [14] Sébastien Krut, Olivier Company and François Pierrot. Force Performance Indexes for Parallel Mechanisms with Actuation Redundancy, especially for Parallel Wire-Driven Manipulators. IEEE IROS 2004: IEEE/RSJ Int. Conf. on Intelligent Robots and Systems, Sendai, Japan, September 28 - October 2, 2004
- [15] Srinivasan, M. y Chen, J., Human Performance in Controlling Normal Forces of Contact with Rigid Objects. Advances in Robotics, Mechatronics and Haptic Interfaces, DSC-Vol. 49, ASME, New York, pp. 119-125, 1993.
- [16] Tan, H., Srivasan, M., Eberman, B., y Cheng, B., Human Factors for the Design of Force Reflecting Haptic Interfaces. Proceedings of ASME WAM, DSC-Vol. 55-1, ASME, New York, pp. 353-360, 1994.